Postprint of: Wielgosz P., Paziewski J., Krankowski A., Kroszczyński K., Figurski M., Results of the application of tropospheric corrections from different troposphere models for precise GPS rapid static positioning. Acta Geophysica, Vol. 60, Iss. 4 (2012), pp. 1236–1257

RESULTS OF THE APPLICATION OF TROPOSPHERIC CORRECTIONS FROM DIFFERENT TROPOSPHERE MODELS FOR PRECISE GPS RAPID STATIC POSITIONING

Paweł Wielgosz[1], Jacek Paziewski[1], Andrzej Krankowski[1],

Krzysztof Kroszczyński[2], Mariusz Figurski[2]

[1]University of Warmia and Mazury in Olsztyn,
Oczapowskiego 1, Olsztyn, Poland
[2]Military University of Technology,
Kaliskiego 2, Warsaw, Poland

e-mails: pawel.wielgosz@uwm.edu.pl, jacek.paziewski@uwm.edu.pl

ABSTRACT. In many surveying applications determination of accurate heights is of significant interests. The delay caused by the neutral atmosphere is one of the main factors limiting the accuracy of GPS positioning and affecting mainly height coordinate component rather than horizontal ones. Static positioning mode provides the most accurate solution relative to other satellite positioning techniques. Estimation of the zenith total delay is a commonly used technique for accounting for the tropospheric delay in static positioning. However, in the rapid static positioning mode the estimation of the zenith total delay may fail since for its reliable estimation longer observing sessions are required. In this paper, several troposphere modeling techniques were applied and tested with three processing scenarios: a single baseline solution with various height differences and a multi-baseline solution. In specific, we introduced external zenith total delays obtained from Modified Hopfield troposphere model with standard atmosphere parameters, UNB3m model, COAMPS numerical weather prediction model and zenith total delays interpolated from a reference network solution. The best results were obtained when tropospheric delays derived from the reference network were applied. The presented analyses concern rapid static positioning and medium scale network (baseline lengths of ~70 km).

KEY WORDS: GPS, rapid static positioning, tropospheric delay, zenith total delay

1. INTRODUCTION

The tropospheric refraction, among other error sources like the ionospheric refraction, multipath and signal obstructions is one of the main factors limiting accuracy of the Global Navigation Satellite Systems (GNSS) measurements. Nowadays, one can observe the increasing demand of reliable, accurate and fast results from precise Global Positioning System (GPS) positioning. GPS technique is commonly used in geodesy, land surveying, civil engineering, deformation monitoring and structural monitoring where precise, centimeter-level accuracy height of sites is often compulsory. Unfortunately the tropospheric refraction is strongly correlated with the vertical coordinate component of a site and affects this component rather than the horizontal ones (Rothacher 2002). Since static relative positioning gives the most accurate coordinates results, this technique is one of the most widely used techniques in precise applications. On the other hand, it requires long observational sessions which are function of baseline length and a number of observed satellites. That is why rapid static positioning technique gains importance. For this type of static positioning efficient carrier phase ambiguity resolution, which require elimination of wave propagation errors, is crucial.

Satellite signals from GPS satellites suffer from the influence of the Earth's atmosphere, which deteriorates the accuracy of the obtained positions. The major part of this phenomenon is caused by the ionized part of the upper atmosphere and is termed as the ionospheric refraction. Fortunately, application of dual (or multi) frequency signals allows GPS users to mitigate this impact (iono-free linear combination removes the first order of ionospheric refration) (Schaer 1999). Additionally, electromagnetic waves are refracted in the neutral, lower part of the Earth's atmosphere. Influence of the neutral atmosphere is commonly referred to as the tropospheric refraction since the 80% of the delay experienced in the layer is caused by troposphere (Hopfield 1971). In detail, GPS signal slows down and its path is getting curved. By contrast to the ionospheric delay, this influence cannot be eliminated using the dual frequency relationship. It is because of non-dispersive nature of the neutral atmosphere for microwave frequencies.

Changes in speed and path cause delay in travel of signal in comparison to travel in vacuum. The delay due to the tropospheric refraction may be expressed (Leick 2004):

$$\delta\rho_{trp} = \int n(s)\ ds - \int ds \tag{1}$$

Where $\delta\rho_{trp}$ is tropospheric delay and $n(s)$ is refractive index as a function of path length. It is common to divide the troposphere into hydrostatic and non-hydrostatic part due to the water vapor content. The tropospheric zenith total delay may be expressed as a sum of hydrostatic (dry) and non-hydrostatic (wet) zenith delays (Equation 2):

$$ZTD = ZHD + ZWD \tag{2}$$

where *ZTD* is total zenith delay, *ZHD* – zenith hydrostatic delay and *ZWD* zenith non-hydrostatic delay.

Significant errors may be introduced when ZTDs are mapped into slant tropospheric delays with mapping functions. Converting (mapping) zenith delays into slant delays with the use of proper and accurate mapping function is of crucial interest because for low elevation angles (<15 degrees) the slant delay is ten times larger than for zenith direction (Ramjee & Ruggieri 2005). The slant total delays toward satellite are computed using the following formula (Equation 3) (Leick 2004):

$$STD(e) = ZHD \times m_d(e) + ZWD \times m_w(e) \tag{3}$$

where:

e – elevation angle towards the satellite,
$STD(e)$ – slant total delay,
ZHD – zenith hydrostatic (dry) delay,
$m_d(e)$ – mapping function for the hydrostatic delay,
ZWD – zenith non-hydrostatic (wet) delay,
$m_w(e)$ – mapping function for the non-hydrostatic delay.

In recent years significant development can be observed in research on troposphere mapping functions. There are a number of simple but less accurate mapping functions like Chao, Black and Eisner, Foelsche and Kirchengast which depend only on elevation angle and are used mainly in navigational applications (Guo, 2003). On the other hand, there are also more sophisticated mapping functions used in precise positioning like Davis, Herring, and Niell, which often depends also on meteorological parameters. Nowadays the best results provide troposphere mapping functions derived from numerical weather models (NWMs) like VMF1 (Vienna Mapping Function) or empirical GMF – (Global Mapping Function) based on the former (Boehm et al. 2006, Steigenberger et al. 2009). Modern functions allow mapping ZTD for very low elevation angles, even down to 2 degrees (Guo, 2003, Boehm 2006, Vey 2006, 2007a, 2007b, Saha et al. 2010).

2. ZENITH TOTAL DELAY MODELING

In order to achieve required highest level of precision of determined coordinates in static relative positioning, it is necessary to use appropriate troposphere modeling techniques. When processing medium and long baselines, especially in mountainous area, site specific tropospheric parameters decorrelate and double-differencing of GPS observations cannot reduce neutral atmospheric effects. What is more, also simple troposphere models can fail in these conditions. Generally, two main groups of tropospheric modeling strategies are in use for mitigating tropospheric delay in precise relative static GPS positioning: (1) zenith total delay estimation from actual observations and (2) providing external corrections (Bock and Doerflinger 2000). The first technique assumes in specific to model hydrostatic zenith delay and to estimate zenith non-hydrostatic delay for GPS sites as parameter in post-processing simultaneously with other parameters (eg. coordinates, ambiguities). This technique is the most widely used strategy for tropospheric modeling, and allows the highest accuracy. Unfortunately, for reliable ZTD estimation, a change in satellite geometry is needed (which means longer session). Additionally, by the reason of high troposphere correlation between nearby stations, ZTDs are mainly estimated in medium and large scale GPS networks with baselines exceeding 100 km. In processing large scale networks it is recommended not only to estimate ZTD, but also horizontal gradients in order to account for neutral atmosphere asymmetries.

When processing local networks (or single, short baselines), in rapid/fast static mode it is not feasible to estimate ZTD. The easiest way to mitigate the tropospheric delay is to use well-known, tropospheric global prediction models like: Hopfield, Modified Hopfield or Saastamoinen with standard or in situ collected or obtained from models like GPT (Global Pressure and Temperature, Boehm et al. 2007a) meteorological parameters. These simple models depend on the location of a station and external meteorological parameters like pressure, temperature and humidity. However, one must note that while hydrostatic tropospheric delays derived from such models are reliable and sufficiently accurate, non-hydrostatic tropospheric delay may be charged with higher error (Mendes 1999). This is because of the non-linear and non-homogenous distribution of water vapor in the neutral

atmosphere, which is crucial for the ability to model non-hydrostatic tropospheric delay. Fortunately it is assumed that hydrostatic tropospheric delay is responsible of about 90% of total delay. Another troposphere modeling strategy is to use hybrid neutral atmosphere delay model like UNB3m. This model uses the Saastamoinen model to compute ZTD and Niell mapping function for the calculation of STD (Leandro 2008). In the contrary to earlier simplified models it depends not only on location of site but also on the day of year which is needed for the prediction of meteorological parameters. Meteorological parameters at specified day of year and at site location (latitude and height) are obtained with the use of look-up table for mean and amplitude together with cosine function for the annual variation and interpolation for latitude (Leandro 2006, Leandro 2008). These kinds of models might be useful especially in real time or rapid static positioning or anywhere where in situ meteorological parameters are not available.

The relationships between meteorology and GPS positioning are getting tight. Combining GPS positioning with Numerical Weather Prediction models, which characterize 3D state of the neutral atmosphere in structures of series of pressure levels, may have bilateral benefits. GPS derived Precipitable Water Vapor (PWV) may be an additional source of data for the NWP in order to forecast the weather. Researches show that introduction of GPS-derived PWV evidently improves short term weather forecast (Gutman 2001). On the other hand NWP may be used in GPS positioning for obtaining meteorological parameters at GPS site, deriving zenith total delays, slant total delay, vertical gradients and developing new mapping functions. Application of NWP in GPS precise positioning is nowadays of specific interest. The concept of application of NWPs models in various positioning techniques has been investigated in several researches. Pany (2001) conducted research where ECMWF numerical weather derived corrections were used to correct GPS observations. Another research results may be found in Jensen (2002) where DMI-HIRLAM-E numerical weather model was applied in static and kinematic mode. Bisnanth et al. (2004) and Zhang and Barton (2005) have introduced external NOAA derived tropospheric correction in DGPS network. Ahn et al. (2006) have analyzed introduction of NOAA NWP model in RTK positioning. Some researchers have shown that however NWPs derived slant tropospheric delays are not good enough to improve accuracy of GPS positioning, they can be used to obtain tropospheric delay gradients (Ghoddousi-Fard et al 2009), another attempt of application of NWM derived slant delays in PPP was made by (Hobiger 2008b). The drawback of the application of NWPs in GPS positioning are still the computational difficulties.

Establishment of dense ground GNSS permanent networks gives the opportunity to generate local or regional ZTD fields. Continuously operating GPS reference networks deliver ZTD at CORS stations which can be interpolated to the user receiver location. This solution require not only spatial but also temporal interpolation, since most frequently active control networks provide ZTD with 1-hour temporal resolution as it is in the Polish part of the European Position Determination System – ASG-EUPOS (Bosy 2007).

The motivation of this research was to investigate the influence of different troposphere modeling techniques in rapid static positioning when estimation of ZTD may fail and when in situ meteorological observations are not available. In specific, we examined introduction of zenith total delay from selected external, very different sources described below (Section 3). In this order processing experiment, briefly discussed below, was carried out. The study presented here concern medium scale network and rapid static positioning with 10-minute long data spans. As a result the position repeatability (especially height component) of determined rover station will be analyzed. A standard deviation of the time series of coordinates obtained from processing of all the sessions served here as a measure of the repeatability. The coordinate residuals with respect to the reference coordinates of the user

station were also analysed. All the processing computations were performed using GINPOS software developed by the authors at the University of Warmia and Mazury in Olsztyn.

3. EXPERIMENT

3.1. TEST DATA

For our experiment we used GPS data from the southern part of the ASG-EUPOS network. ASG-EUPOS is the Polish part of the European Position Determination System (EUPOS), which is an active reference network that provides variety of services for geodesy, surveying and navigation (Bosy 2007). In specific, we chose reference stations located in the Carpathian Mountains with height differences up to several hundreds of meters (Figure 1). This localization was chosen for its representation of area with reference stations located at different heights with respect to the user receiver. Short data spans (10 minutes) were used to process medium-length baselines (~70 km). Equipment of the reference stations consist of: ASHTECH UZ-12 receiver with choke ring antenna ASH701945C_M SNOW at KRAW station, Trimble NetRS receivers at LELO, ZYWI and NWTG stations with Trimble Zephyr Geodetic w/Radome (TRM41249.00 TZGD) antenna at LELO station, Trimble Choke Ring w/SCIT Dome (TRM29659.00 SCIT) at NWTG station and Trimble Zephyr GNSS Geodetic II w/Radome (TRM55971.00 TZGD) at ZYWI station.

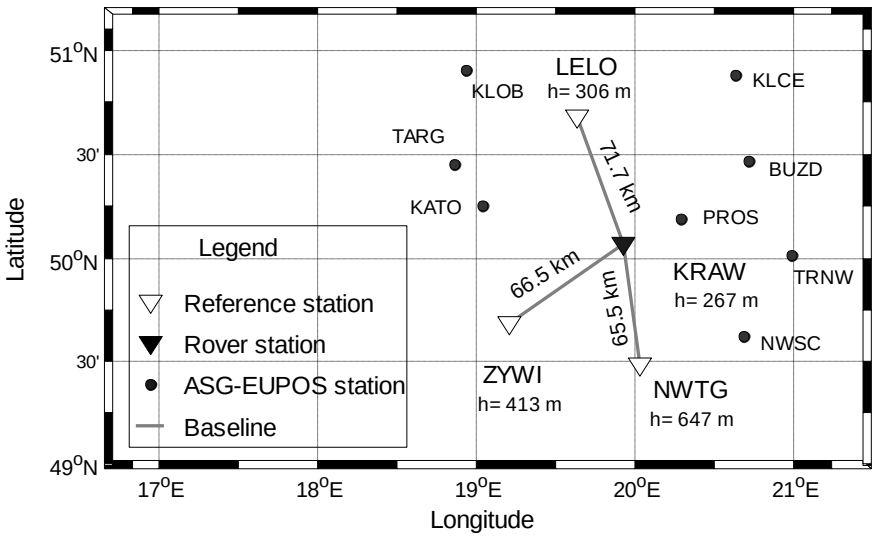

Fig. 1. The baselines processed in the experiment

We made use of dual-frequency pseudorange and carrier phase GPS data. 24 hours of GPS data from ASG-EUPOS network, collected on 10 June 2009 with 60 s interval, were divided into 10-minute sessions starting every 10 minutes. Total number of 144 sessions per baseline was processed in order to analyze accuracy and repeatability of the derived rover station coordinates. KRAW station was selected as a simulated user receiver (rover), LELO, NWTG, ZYWI served as reference stations. Three baselines with different height differences ranging from 39 m to 379 m and lengths ranging from 65 to 72 km were formed (Figure 1). ZTDs derived from different, analyzed models were mapped into slant delays using the GMF function and applied to correct the GPS observations. Although these height differences are not very large, they are the largest available in Polish part of EUPOS.

3.2. PROCESSING SCENARIOS

In order to analyze applicability of different strategies of zenith total delays modeling we processed a baseline with stations at similar height (Scenario 1) and another one with maximal available height difference (Scenario 2) (Table 1). The two chosen baselines were processed independently. Since the tropospheric delay mostly impacts the height component, processing baselines with significant height differences may help to validate ZTD modeling techniques in rapid static positioning. We may expect that when processing the baseline with small height difference the impact of the troposphere modeling techniques on coordinates' domain will be the smallest. In addition a multi-baseline (network) solution with three baselines was also carried out (Scenario 3).

Table 1 Lengths and height differences (ΔH) of the processed baselines

Baseline	Length	Δ H
KRAW-LELO	71.7 km	39 m
KRAW-NWTG	65.5 km	379 m
KRAW-ZYWI	66.5 km	146 m

In all scenarios dual-frequency pseudorange and carrier phase observations (GPS L1&L2) were used. The LAMBDA Least-squares AMBiguity Decorrelation Adjustment method (Teunissen 1994; de Jonge and Tiberius 1996) was applied for ambiguity resolution. The ionospheric delay was modeled by estimation of double differenced ionospheric delay (as parameters with constraints of 0.10 m). A detailed description of the applied strategy of the ionospheric delay estimation may be found in (Wielgosz 2010). It was sufficient for this length of baselines (no exceeding 72 km) to use broadcast ephemerides. In the processing, absolute antenna phase center variations and offsets according to IGS (International GNSS Service) standards were applied.

In general observations from low elevation angle satellites help to decorrelate height and ZTD in least squares estimation. On the other hand these observations introduce higher noise. In this experiment ZTDs were derived from the selected models and used as corrections in the least squares (so no ZTD estimation took place). Hence, the cut-off angle was set up to 10 degrees. A 1/sin(e) function was applied for weighting the observations in least squares estimation with respect to the elevation angle (e). Coordinates of the reference sites were constrained to 2 mm (both horizontal and vertical components). Different troposphere modeling techniques described briefly below were used to provide ZTDs and eliminate tropospheric refraction from GPS data in the processing. In order to assess the results, we adopted the coordinates derived with the Bernese 5.0 software using data from three 24-hour sessions as a reference position of the user receiver.

3.3. TESTED STRATEGIES OF TROPOSPHERIC DELAY MODELING

This contribution presents performance assessment of several different troposphere modeling techniques providing ZTD for precise rapid-static positioning. We intentionally selected techniques that model troposphere in a completely different way. GINPOS software has been employed in four strategies of troposphere modeling techniques assuming using:

Strategy 1: **Modified Hopfield** model (Goad & Goodman 1974) with standard atmosphere parameters;

Strategy 2: **UNB3m** model (Leandro et al. 2008);
Strategy 3: **COAMPS** (The Coupled Ocean/Atmosphere Mesoscale Prediction System, Hodur et al. 2002) numerical weather prediction model. It was used to provide the tropospheric ZTD;
Strategy 4: EUPOS network-derived ZTD interpolated to the user location (referred hereafter **EUPOS**).

In the first strategy we applied well-known and commonly used Modified Hopfield model with standard atmosphere parameters (temperature 18.5 Celsius, pressure 1013.25 hPa, relative humidity 50% at the sea level) and internal mapping function, assuming that the user has no access to in situ meteorological data.

The second strategy employs UNB3m model (developed at the University of New Brunswick) only to obtain zenith total delays. Specifically, in this strategy, ZTD is predicted using Saastamoinen model with meteorological parameters obtained with the use of look-up table together with cosine function for the annual variation and interpolation for latitude (Leandro et al. 2008).

In the third strategy – COAMPS – ZTDs were obtained for every site using ray-tracing solving Eikonal equation (Hobiger 2008a) through numerical weather prediction model in zenith direction. The COAMPS (Coupled Ocean/Atmosphere Mesoscale Prediction System) model with the spatial resolution of 1.44 km and 1 hour time step and 30 horizontal levels, which is currently tested at the Centre for Applied Geomatics of the Military University of Technology in Warsaw, Poland (CGS-WUT), was used in this research (Figurski et al. 2009). The model is built of four components which are: quality control of different sourced observations, analysis with the interpolation to the regular grid, model initialization and the numerical forecast model (Hodur et al. 2002). The advantage of the COAMPS is that the grid spacing may be set to any desirable size. A linear interpolation algorithm was used to generate ZTD for every processed session from 1h spaced ZTDs derived from COAMPS.

In the last strategy – EUPOS – we make use of network derived ZTDs. The ZTD for the user receiver was interpolated temporally (since ZTDs were provided in 1h time span) using linear interpolation and spatially (using ordinary 2D kriging interpolation of ZTD at sea level) from official EUPOS network solution. In last three strategies (Strategy 2, 3 and 4) we mapped ZTD into STD using GMF function.

To get the first impression on how different sources of ZTDs compare with each other, Figure 2 presents ZTDs for KRAW station (rover), obtained by using different modeling techniques. Additionally "true" ZTD (estimated in EUPOS network solution from GPS observations) at KRAW station was plotted. As Figure 2 has shown, there are significant offsets between the actual ZTD derived from GPS observations and obtained from COAMPS numerical weather model. Similar conclusion was draw by Hobiger et al. 2010, where CReSS (Cloud Resolving Storm Simulator) fine-mesh and MANAL (Mesoscale Analysis Data) meso-scale numerical weather models were used. One can see that Modified Hopfield an UNB3m ZTD are constant since the first one depends only on the location of station and second one additionally depends on the day of year. COAMPS, Modified Hopfield and UNB3m derived ZTDs show bias in respect to the ZTDs estimated in the network processing (which may be regarded as the most reliable). The ZTD interpolated from the neighboring ASG-EUPOS stations shows the best agreement.

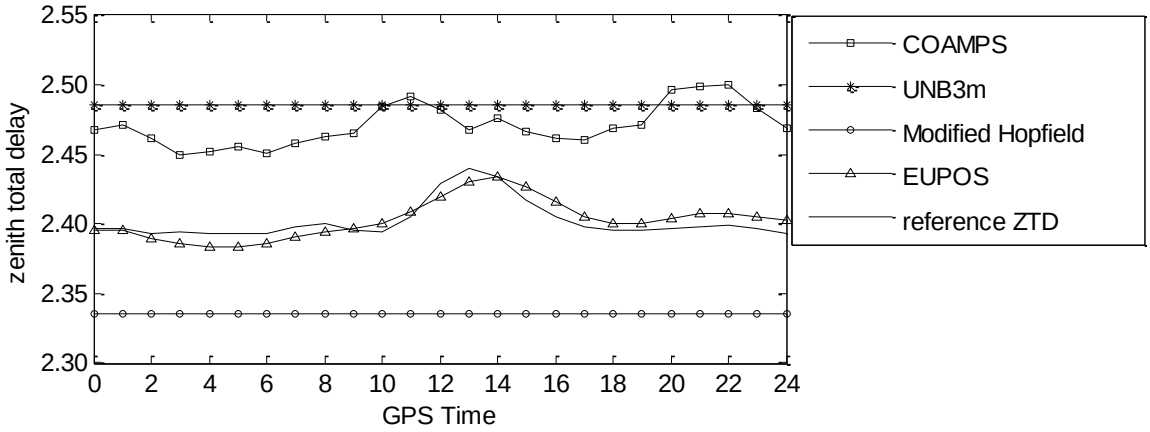

Fig. 2. Zenith total delays from different sources for KRAW station used in processing in the experiment.

3.4. TESTS RESULTS – SCENARIO 1 - SINGLE BASELINE WITH STATIONS AT SIMILAR HEIGHT

In this section, the results of processing of single baseline KRAW-LELO with small height difference are presented. Application of ZTD from analyzed models mostly affected height rather than horizontal coordinates (Table 2). There was no considerable effect of troposphere modeling technique on horizontal components. Standard deviations (dispersion) of horizontal components were always below 10 mm. Introduction of Modified Hopfield model, UNB3m or EUPOS network derived ZTD resulted in similar height and horizontal coordinates' accuracy. In specific, introduction of Modified Hopfield model with internal mapping function resulted in standard deviation of height of 36 mm with mean residual of 0 mm (with respect to the reference position). Similar accuracy were obtained using UNB3m model with standard deviation of 36 mm and mean residual of 7 mm, and for EUPOS derived ZTDs with std of 30 mm, mean residual of 4 mm. Slightly worse results were achieved when using COAMPS numerical weather model derived ZTDs, where standard deviation and mean of height were respectively of 50 mm and 3 mm. Detailed statistics of the results from the first scenario are presented in Table 2.

Table 2. Standard deviations and mean of coordinate residuals (in mm) obtained when processing KRAW-LELO baseline – scenario 1.

Strategy		**Modified Hopfield**	**UNB3m**	**COAMPS**	**EUPOS**
N	***std***	9	9	10	8
	mean	-3	-4	-5	-5
E	***std***	8	8	9	8
	mean	-3	-2	-3	-2
U	***std***	36	36	50	30
	mean	0	7	-4	3

In Figures 3-6, there are presented scatter plots of rover height residuals to the reference height. As it can be seen in the figures, the height residuals for Strategies 1-3 show similar variability. The height components obtained by using EUPOS interpolated ZTDs are the most

constant in time and vary around the reference value. Almost all the determined heights are located within +/- 50 mm in respect to the reference height.

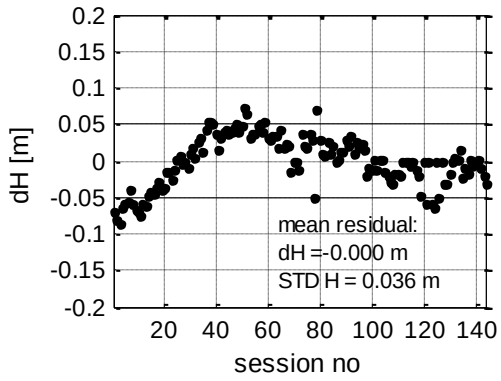

Fig. 3. Rover height residuals for KRAW-LELO baseline obtained using Modified Hopfield model.

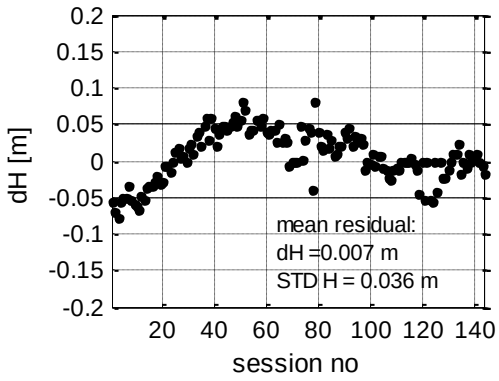

Fig. 4. Rover height residuals for KRAW-LELO baseline obtained using UNB3m model.

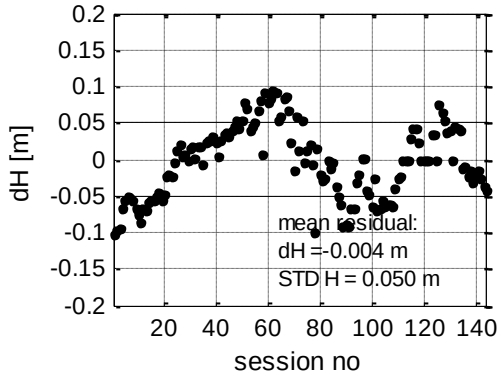

Fig. 5. Rover height residuals for KRAW-LELO baseline obtained using COAMPS derived ZTDs.

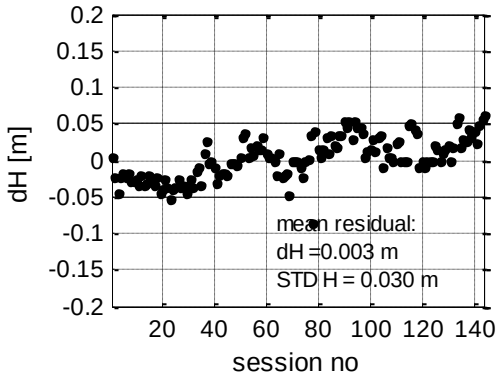

Fig. 6. Rover height residuals for KRAW-LELO baseline obtained using EUPOS derived ZTDs.

The height residual histograms can be found in Figures 7-10. For network derived ZTDs (EUPOS) 85% of height residuals were smaller than 50 mm. The worst results were obtained using COAMPS derived ZTDs. In this scenario 44% of the height residuals were greater than 50 mm. In case of the application of Modified Hopfield and UNB3m models 76% and 75% of the residuals were below 50 mm respectively.

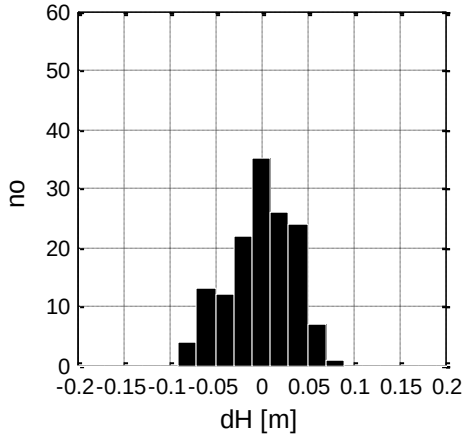

Fig. 7. Rover height residual histogram for KRAW-LELO baseline obtained using Modified Hopfield model.

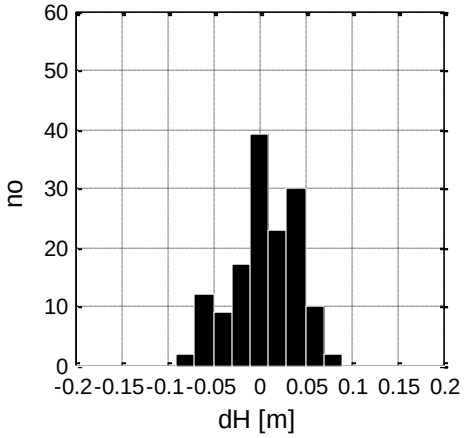

Fig. 8. Rover height residual histogram for KRAW-LELO baseline obtained using UNB3m model.

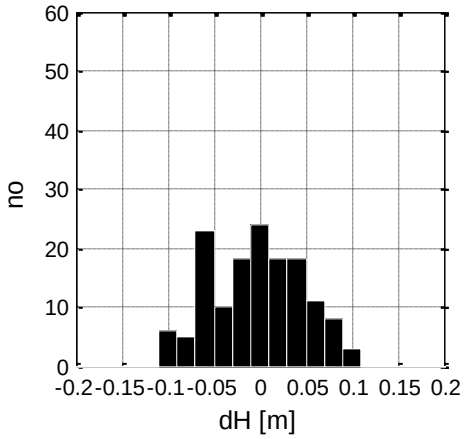

Fig. 9. Rover height residual histogram for KRAW-LELO baseline obtained using COAMPS derived ZTDs.

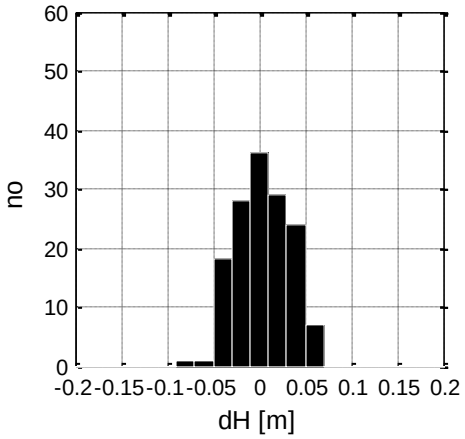

Fig. 10. Rover height residual histogram for KRAW-LELO baseline obtained using EUPOS derived ZTDs.

Figure 11 shows empirical cumulative distribution functions (cdf) of the height error obtained applying the analyzed models. These results indicate that application of EUPOS-derived ZTDs in rapid static positioning may result in the height accuracy of the order of several centimeters. Empirical cumulative distribution functions of the height error for Modified Hopfield and UNB3m show similar shapes, while cdf for COAMPS indicates significantly lower accuracy with respect to the other strategies at the same confidence level.

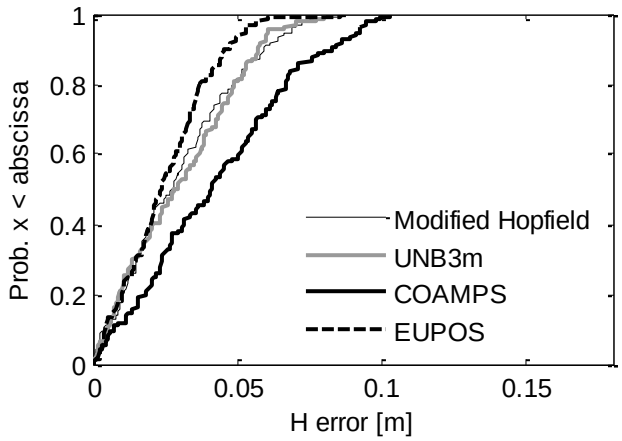

Fig. 11. Cumulative distribution function of KRAW station height error obtained applying different tropospheric modeling strategies for KRAW-LELO baseline processing.

3.5. TESTS RESULTS – SCENARIO 2 - SINGLE BASELINE WITH STATIONS AT DIFFERENT HEIGHTS

Next analyses present results of processing KRAW-NWTG baseline with much larger height difference of 379 m. The more challenging conditions for GPS processing may enhance the influence of neutral atmosphere modeling on the positioning results. We expect that differences between the strategies should be more significant due to larger residuals tropospheric delay in double-differenced observations. For the sake of comparison standard deviations and mean residuals of the coordinates of rover obtained from KRAW-NWTG baseline are presented in Table 3.

Table 3. Standard deviations and mean of coordinates residuals (in mm) obtained when processing KRAW-NWTG baseline – scenario 2.

Strategy		**Modified Hopfield**	**UNB3m**	**COAMPS**	**EUPOS**
N	***std***	10	10	11	10
	mean	2	3	4	4
E	***std***	9	9	9	8
	mean	-4	-4	-4	-5
U	***std***	51	51	56	32
	mean	-10	-3	-23	2

The best results were again obtained for the EUPOS network derived ZTDs, likewise when processing KRAW-LELO baseline. And again the influence of the strategy selection on the horizontal coordinates was rather insignificant. Figures 15 and 19 show good results for this approach. Standard deviation and mean residual for height are the smallest using EUPOS derived corrections in this scenario. Other approaches are characterized by similar standard deviations of height which lie in the range of 51-56 mm, however COAMPS strategy shows the largest shift in respect to the reference height - 23 mm. In Figures 12-14, in the middle of the processed time span, one can notice significant decrease of the height accuracy (height residuals reach over -0.15 m) when applying COAMPS corrections, which is not observed when applying EUPOS corrections (Figure 15). Maximal height residuals for EUPOS strategy reach approximately - 0.09 m.

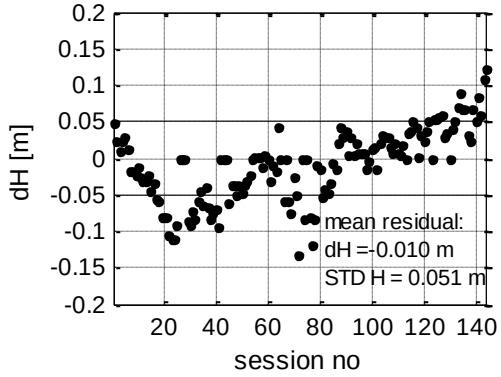

Fig. 12. Rover height residuals for KRAW-NWTG baseline solution with Modified Hopfield model.

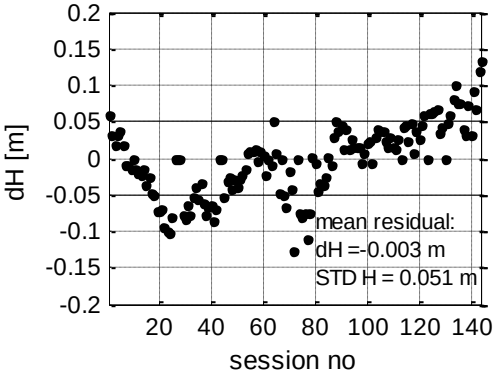

Fig. 13. Rover height residuals for KRAW-NWTG baseline solution with UNB3m model.

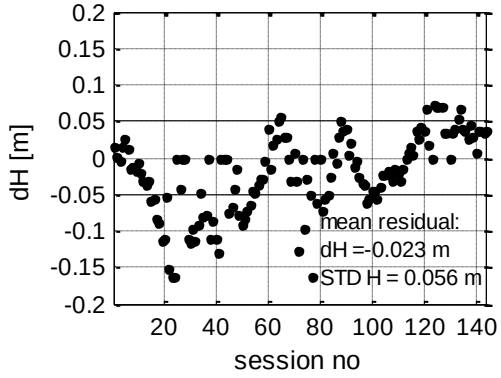

Fig. 14. Rover height residuals for KRAW-NWTG baseline solution with COAMPS derived ZTDs.

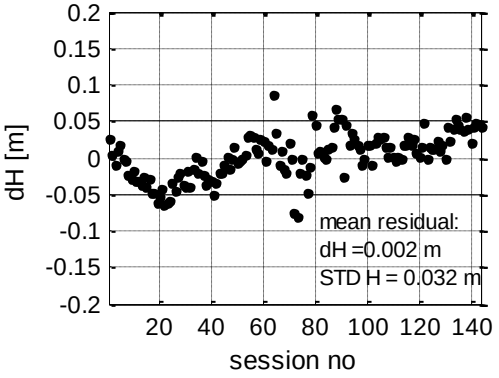

Fig. 15. Rover height residuals for KRAW-NWTG baseline solution with EUPOS derived ZTDs.

In Figures 16-19 one can see height residual histograms when applying specified strategies to the KRAW-NWTG baseline processing. For EUPOS network derived ZTDs 87% of height residuals were smaller than 50 mm, other strategies indicated similarly lower percentage of height residuals smaller than 50 mm: Modified Hopfield 58%, UNB3m 60%, COAMPS ZTDs 59%.

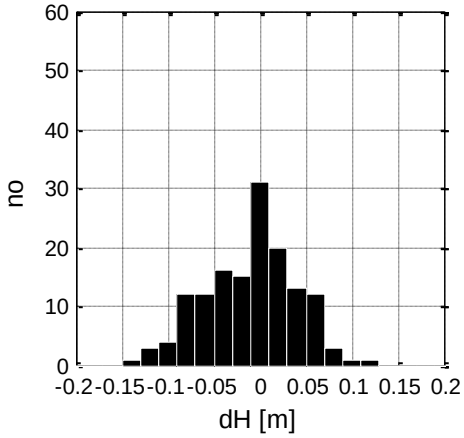

Fig. 16. Rover height residual histogram for KRAW-NWTG baseline solution with Modified Hopfield model.

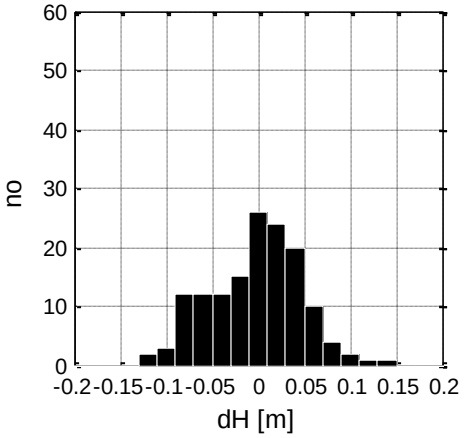

Fig. 17. Rover height residual histogram for KRAW- NWTG baseline solution withUNB3m model.

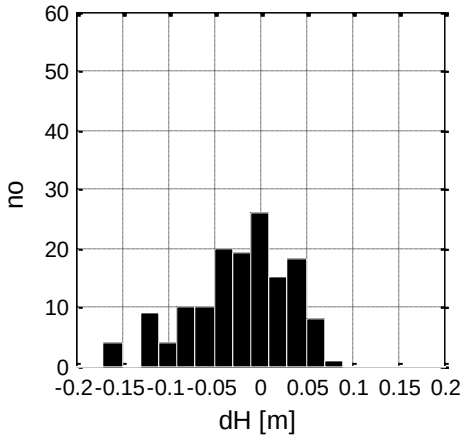

Fig. 18. Rover height residual histogram for KRAW- NWTG baseline solution with COAMPS derived ZTDs.

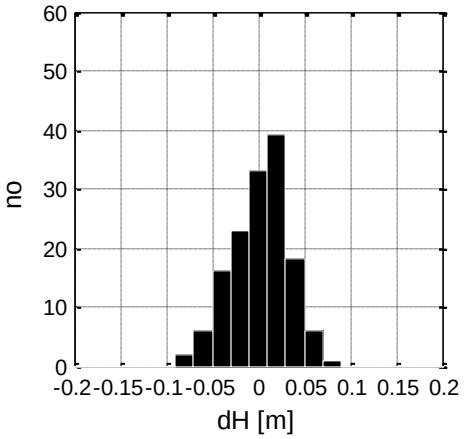

Fig. 19. Rover height residual histogram for KRAW- NWTG baseline solution with EUPOS derived ZTDs.

Figure 20 shows the height error cumulative distribution function that confirms that the application of the network derived ZTDs for troposphere delay mitigation provides the best results. Application of the other strategies results in similar shape of the cumulative distribution function.

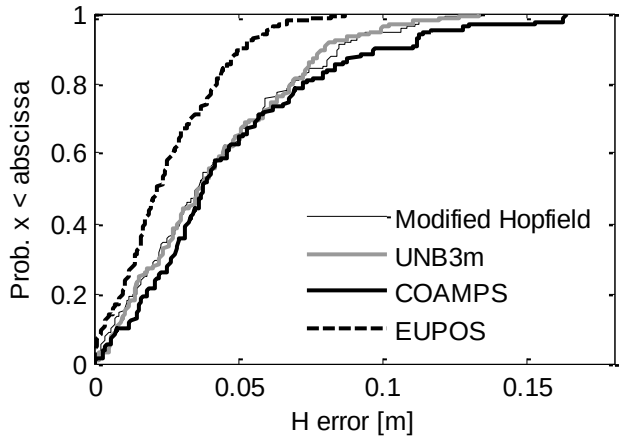

Fig. 20. Cumulative distribution function of rover height error obtained when applying different tropospheric modeling for KRAW-NWTG baseline processing.

3.6. TESTS RESULTS – SCENARIO 3 - MULTI-BASELINE SOLUTION

Finally, below there is presented performance of multi-station processing. In this approach all mathematical correlations between the observations from all the baselines are taken into account in the common adjustment. The same troposphere modeling techniques as in the single-baseline case were applied and tested. Due to the greater number of observations, the position accuracy and repeatability is expected to be higher. Standard deviations of vertical component improved significantly for all of the tropospheric modeling strategies (comparing to a single baseline mode). Application of the corrections from Modified Hopfield, UNB3m and EUPOS shows similar standard deviation of the coordinates (26-27 mm for heights) and similar mean height residual (4-12 mm). Application of the network interpolated ZTDs (EUPOS) resulted in the smallest shift (4 mm) of mean height residual in respect to the reference height (Table 4).

Table 4. Standard deviations and mean of coordinates residuals (in mm) obtained when processing multi-baseline solution – scenario 3.

Strategy		**Modified Hopfield**	**UNB3m**	**COAMPS**	**EUPOS**
N	***std***	8	9	8	7
	mean	-2	-2	-2	0
E	***std***	8	8	8	6
	mean	-5	-5	-4	-4
U	***std***	26	26	32	27
	mean	7	12	23	4

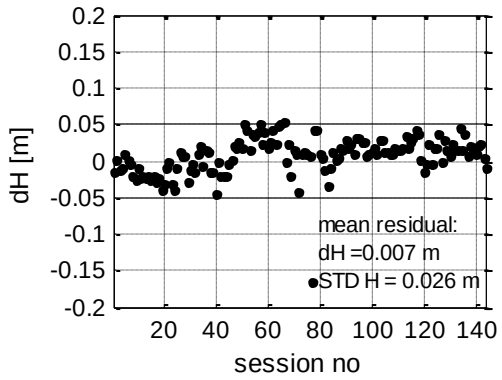

Fig. 21. Rover height residuals for multi-baseline solution with Modified Hopfield model.

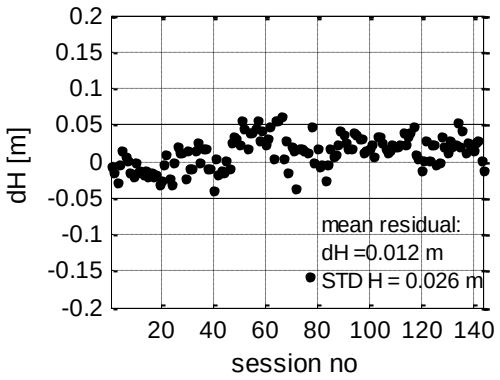

Fig. 22. Rover height residuals for multi-baseline solution with UNB3m model.

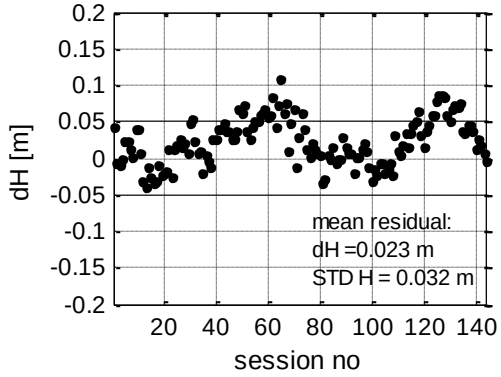

Fig. 23. Rover height residuals for multi-baseline solution with COAMPS derived ZTDs.

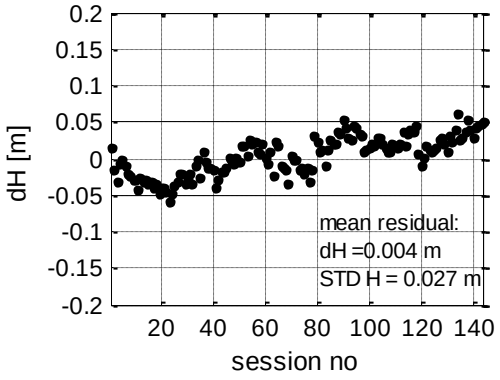

Fig. 24. Rover height residuals for multi-baseline solution with EUPOS derived ZTDs.

Again, Modified Hopfield, UNB3m and EUPOS indicate similar percentage (94-96 %) of height residuals smaller than ±50 mm, which is ~36% better comparing to the results of the KRAW-NWTG baseline processing (Scenario 2). One must remember that in the multi-baseline solution the baselines with height differences ranging from 39 to 379 meters were processed. In Figures 25-28 one can see height residual histograms when applying specified strategies to the multi-station processing. For the EUPOS network derived ZTDs and Modified Hopfield model 96% of height residuals were smaller than ±50 mm. For the UNB3m model 94% of the residuals did not exceed this limit. For COAMPS-derived ZTDs only 78 % of height residuals were within ±50 mm limit.

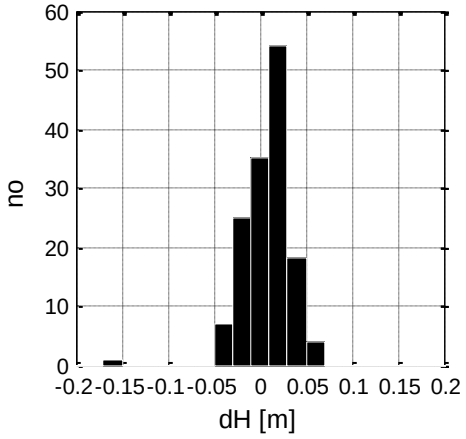

Fig. 25. Rover height residual histogram for multi-baseline solution with Modified Hopfield model.

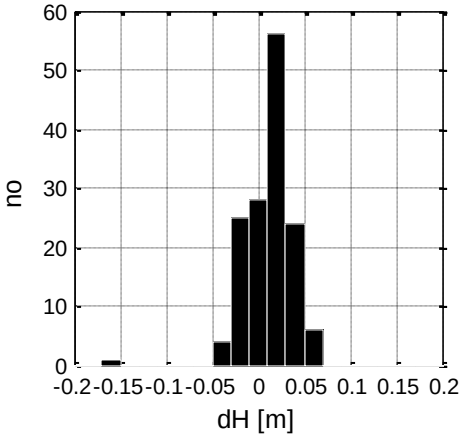

Fig. 26. Rover height residual histogram for multi-baseline solution with UNB3m model.

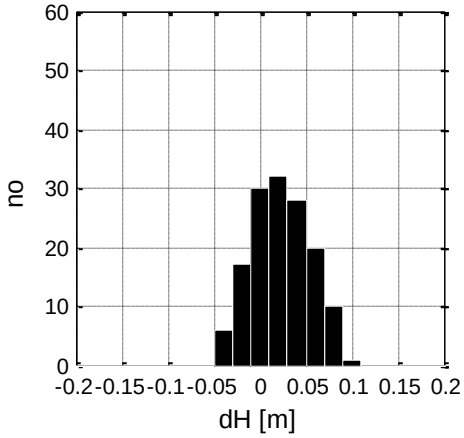

Fig. 27. Rover height residual histogram multi-baseline solution with COAMPS derived ZTDs.

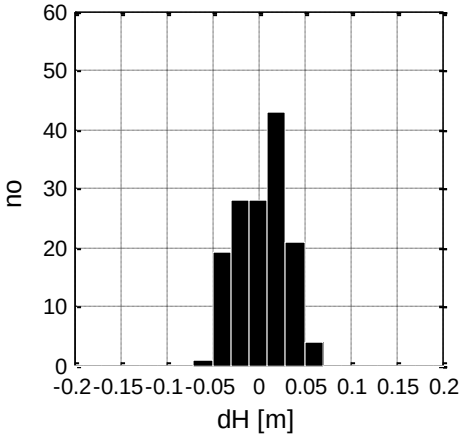

Fig. 28. Rover height residual histogram for multi-baseline solution with EUPOS derived ZTDs.

As shown in Figure 29 ZTDs derived from EUPOS network and interpolated to user proved again to be the best tropospheric modeling technique for rapid static positioning

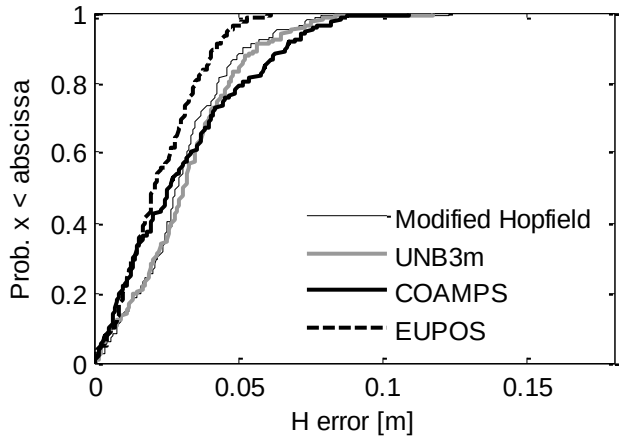

Fig. 29. Cumulative distribution function of rover station height error obtained applying different tropospheric modeling for multi-baseline solution.

However, in the third scenario the influence of the troposphere modeling strategies on the coordinate's domain was less pronounced as in the previous processing scenarios (1, 2). The difference between the highest (COAMPS) and lowest (EUPOS) standard deviation of height coordinate was 23%, while in second scenario this difference between the worst (COAMPS) and best (EUPOS) standard deviation amounted to 43%.

4. CONCLUSIONS

In this work, we made an attempt to compare and validate various techniques for accounting for tropospheric delay in rapid static positioning in medium scale network. From overall performance we conclude that the application of the interpolated reference network-derived ZTDs for user station is the most suitable approach, not only when processing single baseline, but also in multi-baseline solution. Application of network-derived tropospheric corrections

(EUPOS) gave the most accurate coordinates, both horizontal and vertical. In every processing scenario application of ZTDs interpolated from EUPOS network resulted in very similar standard deviation of height in range of 27 to 32 mm (1-sigma confidence level).

Application of standard global troposphere models like Modified Hopfield with standard meteorological parameters or hybrid models like UNB3m taking into account seasonal variations of meteorological parameters at particular location indicated similar level of height precision (26-51 mm). These models still provide reliable results on level sufficient for many of surveying application.

The worst results were obtained when ZTDs was derived from COAMPS numerical weather prediction model. This fact may be caused by insufficient spatial resolution of COAMPS model for this type of area (mountains). It is comparable with earlier studies (Hobiger 2008b) which conclude that NWM derived ZTD need to be used with additional estimation of residual delays.

Multi-baseline (network) solution provided overall the best results in respect to the other processing scenarios. The height coordinate residuals usually fell within +/- 50 mm limit.

We did not observe any important influence of the applied troposphere modeling technique on horizontal coordinates' accuracy in the presented tests. In every processing scenario (single baseline, multi-baseline) and for every troposphere modeling strategy the mean of the residuals of the horizontal components did not exceed ±5 mm, and their standard deviation did not exceed ±11 mm.

Acknowledgements This research was supported by ESA PECS project no. c98094 and grant N526 191937 from the Polish Ministry of Science and Higher Education. The authors are very grateful to the Centre of Applied Geomatics of Military University of Technology for providing Zenith Total Delays from COAMPS numerical weather prediction model.

REFERENCES

Ahn Y. W., Lachapelle G., Skone, S., Gutman S., Sahm, S., (2006) Analysis of GPS RTK performance using external NOAA tropospheric corrections integrated with a multiple reference station approach. *GPS Solutions*, Vol 10, Number 3 / July, 2006, pp. 171-186.

Bisnanth, S. B., Dodd, D., Cleveland, A., Parsons, M., (2004) Analysis of the utility of NOAA-generated tropospheric refraction corrections for the next generation nationwide DGPS service. *Proceeding of ION GNSS 2004*, Long Beach, pp.1288-1297.

Bock O, Doerflinger E, (2000) Atmospheric processing methods for high accuracy positioning with the Global Positioning System, *COST-716 Workshop, Soria Moria*, Oslo (N), July 10-12, Laboratoire OEMI, IGN-SR 00-003/L-COM-OB.

Boehm, J., Werl, B., Schuh, H., (2006) Troposphere mapping functions for GPS and very long baseline interferometry from European Centre for Medium-Range Weather Forecasts operational analysis data. *J Geophys Res*, 111:B02406.

Boehm, J., Heinkelmann, R., Schuh, H., (2007) Short note: a global model of pressure and temperature for geodetic applications. *J Geod*, 81(10), pp. 679-683.

Boehm, J., Mendes Cerveira, P. J., Schuh, H., Tregoning, P., (2007) The impact of tropospheric mapping functions based on numerical weather models on the determination of geodetic parameters. In: Tregoning

Tregoning P, Rizos C. (eds) (2007) *Dynamic planet-monitoring and understanding a dynamic planet with geodetic and oceanographic tools.* Springer, International Association of Geodesy Symposia, 130,pp. 837-843.

Bosy, J., Graszka, W., Leonczyk, M., (2007) ASG-EUPOS—a multifunctional precise satellite positioning system in Poland. *Eur J Nav* Vol 5(4):30–34.

Dach, R., Hugentobler, U., Fridez, P., Meindl, M., (2007) Bernese GPS Software Version 5.0. Astronomical Institute University of Bern, Bern. 364 pages.

Figurski M., Gałuszkiewicz M., Kamiński P., Kroszczyński K. (2009) Mesoscale anisotropy of GPS slant delay. Bulletin of Geodesy and Geomatics, 2/2009, pp 99-110.

Ghoddousi-Fard, R., Dare, P., Langley, R. B., (2009) Tropospheric delay gradients from numerical weather prediction models: effects on GPS estimated parameters. *GPS Solutions.* Vol 13, No 4, pp.281-291.

Goad, C. C., Goodman L., (1974) A Modified Hopfield Tropospheric Refraction Correction Model. American Geophysical Union Annual Fall Meeting, San Francisco, California, December 12–17, pp. 28.

Gutman, S. I., Benjamin, S. G., (2001) The Role of Ground-Based GPS Meteorological Observations in Numerical Weather Prediction. *GPS Solutions*, Volume 4, Number 4 / April, 2001, pp. 16-24.

Guo, J. (2003) A New Tropospheric Propagation Delay Mapping Function for Elevation Angles down to 2°, Proceeding of ION GPS/GNSS 2003. 16th International Technical Meeting of the Satellite Division of The Institute of Navigation, Portland, *OR*, 9 – 12 Sept. 2003. pp 386 – 396.

Hobiger, T., Ichikawa, R.,, Koyama Y., Kondo T., (2008a) Fast and accurate ray-tracing algorithms for real-time space geodetic applications using numerical weather models. *Jurnal of Geophysical research*, Vol. 113, D20302.

Hobiger, T., Ichikawa, R., Takasu, T., Koyama Y., Kondo T., (2008b) Ray-traced troposphere slant delays for precise point positioning. *Earth Planets Space*, Vol. 60 e1-e4.

Hobiger, T., Shimada, S., Shimizu, S., Ichikawa, R., Koyama, Y., Kondo T., (2010) Improving GPS positioning estimates during extreme weather situations by the help of fine-mesh numerical weather models. *Journal of Atmospheric and Solar-Terrestrial Physics.* Vol. 72, pp. 262-270.

Hodur, R. M., Hong, X., Doyle, J. D., Pullen, J., Cummings, J., Martin P., Rennick, M. A, (2002) The Coupled Ocean/Atmosphere Mesoscale Prediction System (COAMPS). *Oceanography*: *The Oceanography Society*: Vol. 15(1), pp. 88-98.

Hofmann – Wellenhof, B., Lichtenegger, H., Wasle, E., (2008) *GNSS – Global Navigation Satellite Systems GPS, GLONASS, GALILEO and more*. Springer, Wien-New York. 516 pages.

Hopfield, H. S., (1971) Tropospheric effect on /electromagnetically measured range: prediction from surface weather data. *Radio Sci*., Vol 6, No. 3, pp. 357-367.

Jensen, A. B. O., (2002) *A Window on the Future of Geodesy* Proceedings of the International Association of Geodesy IAG General Assembly Sapporo, Japan June 30 – July 11, 2003 Springer Berlin Heidelberg, Vol. 128, pp. 65-70.

de Jonge, P. J., Tiberius, C., (1996) The Lambda Method for Integer Ambiguity Estimation: Implementation Aspects. *LGR Publication* No. 12, August, pp. 1–49.

Leandro, R., Langley, R. B., Santos, M. C., (2006) UNB neutral atmosphere models: development and performance. *Proceedings of the Institute of Navigation National Technical Meeting*, 18-20 January, 2006, Monterrey, CA, USA.

Leandro, R. F, Langley, R. B., Santos M. C., (2008) UNB3m_pack: A neutral atmosphere delay package for GNSS. *GPS Solutions*, Vol. 12, No. 1, pp. 65-70.

Leick, A., (2004) *GPS Satellite surveying*. John Wiley&Sons, New Jersey. 474 pages.

Mendes, V. B.. (1999) *Modelling the neutral-atmosphere propagation delay in radiometric space techniques*. Ph.D. dissertation. Department of Geodesy and Geomatics

Engineering. Technical Report no. 199. University of New Brunswick, Fredericton, New Brunswick.
Misra, P., Enge, P., (2006) *Global Positioning System. Signals, Measurements, and Performance*, 2nd ed. Ganga-Jamuna Press, USA, 569 pages.
Niell, A. E., (1996) Global mapping functions for the atmosphere delay at radio wavelengths. *J Geophys Res*, 101(B2):3227-3246.
Ramjee, P., Ruggieri, M., (2005) *Applied satellite navigation using GPS, GALILEO and augmentation systems.* Boston Artech House. Artech House mobile communications series.
Pany, T., Pecec, P., Stangl, G., (2001) Elimination of tropospheric path delays in GPS observations with the ECMWF numerical weather model. *Phys Chem Earth* A 26(6-8), pp.487-492.
Rothacher, M., (2002) Estimation of station heights with GPS. In: Drewes H, Dodson A, Fortes L, Sanchez L, Sandoval P (eds) *Vertical reference systems*. Springer, International Association of Geodesy Symposia, 124:81-90, 228 pages.
Saha, K., Raju, C. S., Parameswaran, K., (2010) A new hydrostatic mapping function for tropospheric delay estimation. *Journal of Atmospheric and Solar-Terrestrial Physics*, Vol. 72, Issue 1, pp. 125-134.
Schaer, S., (1999) *Mapping and Predicting the Earth's Ionosphere Using the Global Positioning System*, Ph.D. dissertation., Astronomical Institute University of Bern, Bern. 205 pages.
Schon, S., Wieser, A., Macheiner, K., (2005) Accurate tropospheric correction for local GPS monitoring networks with large height differences. In *Proc. of ION ITM*, 13-16 Sept. 2005, Long Beach, CA., pp. 250-260.
Schüler, T., (2001). *On ground-based GPS Tropospheric Delay Estimation*, Ph.D. dissertation. Universität der Bundeswehr. Munich. 364 pages.
Seth, I., Gutman, S. I., Benjamin S. G., (2001) The Role of Ground-Based GPS Meteorological Observations in Numerical Weather Prediction. *GPS Solutions*. Vol 4, No 4/April, pp. 16-24.
Steigenberger, P., Boehm, J., Tesmer, V., (2009) Comparison of GMF/GPT with VMF1/ECMWF and implications for atmospheric loading. *J Geod*, 83:943-951.
Teunissen, P. J. G., (1994) A new method for fast carrier phase ambiguity estimation, *Proceedings IEEE PLANS*, Las Vegas, NV, 11–15 April, pp. 562–573.
Teunissen, P. J. G., Kleusberg, A., (1998) *GPS for Geodesy*. Springer - Verlag. Berlin Heidelberg New York. 640 pages.
Vey, S., Dietrich, R., Fritsche, M., Rülke, A., Rothacher, M., Steigenberger, P., (2006) Influence of mapping functions parameters on global GPS network analyses: comparison between NMF and IMF. *Geophys Res Lett* 33:L01814.
Wielgosz, P., (2010) Quality assessment of GPS rapid static positioning with weighted ionospheric parameters in generalized least squares. *GPS Solutions*, DOI 10.1007/s10291-010-0168-6.(accepted for print).
Xu, G., (2007) *GPS, Theory, Algorithms and Applications*. Springer-Verlag. Potsdam. 340 pages.
Zhang, Y., Barton, C., (2005) Comparison of real-time troposphere correction techniques for high performance DGPS application. *Proceeding of ION NTM* 2005, San Diego, pp.666-684.